Int. J. Multiphase Flow Vol. 10, No. 2, pp. 217–228, 1984
Printed in Great Britain.

0301-9322/84 $3.00 + .00
Pergamon/Elsevier

STATISTICAL ANALYSIS OF FLUCTUATIONS OF FROTH PRESSURE ON PERFORATED PLATES WITHOUT DOWNCOMERS

SHIGERU MATSUMOTO and MUTSUMI SUZUKI
Department of Chemical Engineering, Tohoku University, Sendai, Japan

(*Received* 12 *December* 1982; *in revised form* 20 *May* 1983)

Abstract—Statistical properties of fluctuations of pressure drop across the gas–liquid dispersions on the tray were analyzed using a 215 mm dia. three plates column with different trays. Hydrodynamic regimes of the froth were characterized in terms of the statistical properties evaluated. It was proved that the on-line estimation of the flow behavior of the froth was possible on the basis of the pattern recognition of the power spectral density function of the pressure fluctuations. The time-domain stochastic models for fluctuations of the pressure drop were identified so as to be available for its forecast and simulation.

1. INTRODUCTION

It is widely said that the stable operation of sieve plates is not easily attainable because the dynamics of liquid hold-up on the tray is strongly dependent upon the operating conditions such as flow rate of gas and liquid as well as the geometrical configuration of the tray used. There has been, however, published few literatures on this subject especially for sieve trays without downcomers. Shoukry *et al.* (1974a, b) investigated statistically the time-series of the froth pressure drop by using a 300 mm dia. single plate column and defined various hydrodynamic regimes in terms of the statistical properties evaluated.

In usual operations of sieve tray columns, however, there may exist inevitable interactions among the dynamics of froth on the upper and lower plates, and consequently it may be considered that more complicated situations occur. Taking account of the point, we investigate the plate dynamics by using three plates column.

It is desirable in practical operations of sieve tray columns that the hydrodynamics of gas–liquid dispersion on the tray could be monitored and controlled during industrial operations. From such a viewpoint, we examine the possibility of on-line estimation of characteristics of flow regimes and construct the stochastic model of the fluctuations of the froth pressure drop to be used for implementation of controller.

2. EXPERIMENTAL

Figure 1 shows the schematic diagram of plates column used in this experiment. The column is constructed from a 215 mm dia. transparent acrylic tube and three perforated trays are located in the column, with a tray spacing of 300 mm. Two different trays were studied. These trays had 5.0 mm holes, tray I having 13.7% free area while tray II had 8.2% free area. The system air–water at room temperature was used.

Air supplied by a rotary blower is fed into the column through the calming section where its flow rate is measured by means of hot-wire anemometer. Water from overhead tank is measured by orifice meter and fed through the distributer set at the top of the column. Air flow rates ranged from 0.1 to 1.5 m/s, while water flow rates ranged from 3.3×10^{-5} to 5.0×10^{-5} m^3/s.

An arrangement of pressure measurements at several locations is also shown in figure 1. Static pressures in the column were mainly measured by means of semiconductor pressure transducer through a scanning valve, which was controlled by a personal computer. Froth pressure fluctuations, mainly at a point 5 cm from the plate center, were measured by other transducers. The output d.c. voltage corresponding to the pressure signal was at once stored into a transient memory and then it was transferred to a floppy

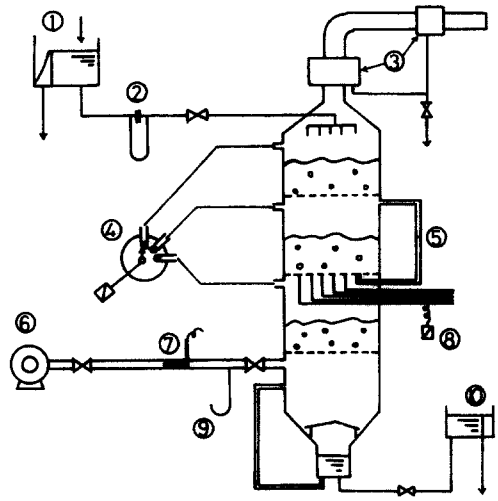

Figure 1. Schematic diagram of experimental apparatus: (1, 10) overhead tank; (2) orifice meter; (3) mist catcher; (4) scanning valve; (5, 9) manometer; (6) rotary blower; (7) hot-wire anemometer; (8) pressure transducer.

disk through a personal computer. After an experimental run, the recorded signals were stored in a file of the mainframe computer (ACOS-1000 system) through an acoustic coupler, and they were analyzed there. Figure 2 is a schematic diagram of the data acquisition system. The transducer systems were calibrated in the preliminary experiment.

3. ANALYSIS OF RANDOM DATA

Sampling rate and length of time series data are important factors for estimation of statistical properties of random data. The former was selected as 100 samples/s so that the Nyquist frequency exceeded the maximum frequency contained in the data which was estimated as 30 Hz according to Shoukry *et al.* (1974a). The latter was 2048 data points, which was chosen on the basis of preliminary experiments and literatures.

Stationarity of time series data was tested based on the nonparametric test suggested by Bendat & Piersol (1971). That is, the time record is divided up so that N representative increments of equal time are obtained. Then a mean square value for each time interval

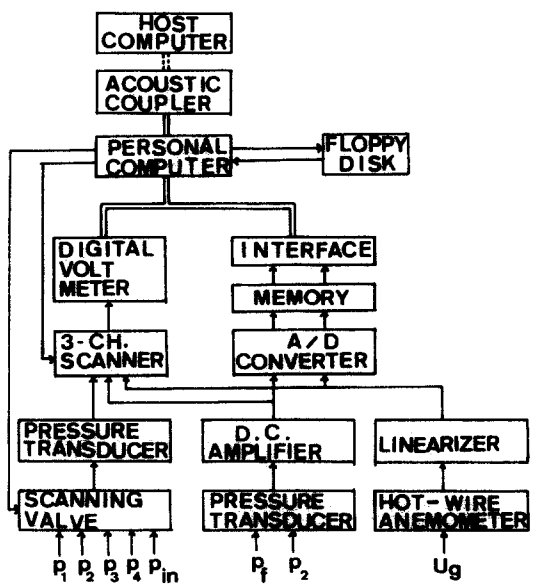

Figure 2. Data acquisition system.

was computed and the results were arranged in sequence: $\bar{x}_1^2, \bar{x}_2^2, \ldots, \bar{x}_N^2$. The run-test was applied for the series around the median value of the mean square. As a result, hypothesis of stationarity was accepted for a significance level of 95%. Thus it was considered that the fluctuations of froth pressure belonged to the class of stationary ergodic stochastic process. On the basis of the ergodic assumption, the statistical parameters of data were evaluated such as the mean value, the variance, the autocorrelation function and the power spectral density function. The procedures are summarized in appendix I. The power spectral density function was evaluated by both FFT method (e.g. Jenkins & Watts 1968) and MEM (maximum entropy method) (e.g. Hino 1977).

Further, the time-domain linear models were developed for the stochastic process. Autoregressive (AR) model and autoregressive and moving average (ARMA) model were applied. Order of the model was determined by the minimum FPE (Final Prediction Error) (e.g. Akaike & Nakagawa 1972) or the minimum AIC (Akaike's Information Criterion) procedure (Akaike 1976). Model parameters were evaluated by the least square estimation. A brief summary of the procedure is presented in appendix II.

4. EXPERIMENTAL RESULTS AND DISCUSSION

4.1 *Liquid hold-up and hydrodynamics of gas–liquid dispersion*

Figures 3 and 4 show the clear liquid height h_L, which corresponds to the liquid hold-up, on the middle plate as a function of superficial air velocity U_G, respectively, with tray I and II, which was measured by means of manometer. In the figures, the hydrodynamic regimes of the gas–liquid dispersions are also indicated in accordance with Shoukry *et al.*'s (1974a) classification. With tray I, the clear liquid height increased linearly with air flow rate up to around 0.7 m/s, and after decreasing gradually thereafter, unstable state occured at about 1.0 m/s. Above an air velocity of 1.2 m/s, the froth on the tray oscillated as a whole and the liquid hold-up dropped rapidly. The oscillation mode was Half-wave oscillation which was distinguished by Biddulph & Stephens (1974). The rapid reduction of hold-up in this regime can be explained by the fact that a portion of very low liquid height appears locally on the tray due to the oscillation and air can blow up through there, resulting in low average hold-up of the froth.

On the other hand, with tray II, a clear oscillating regime was not observed for these liquid flow rates. Above an air velocity of 0.5 m/s, the height of froth expanded up to the upper plate and the flooding occurred. Another noticable feature with tray II is that bubbling regime existed at low air flow rates, while it was not observed with tray I.

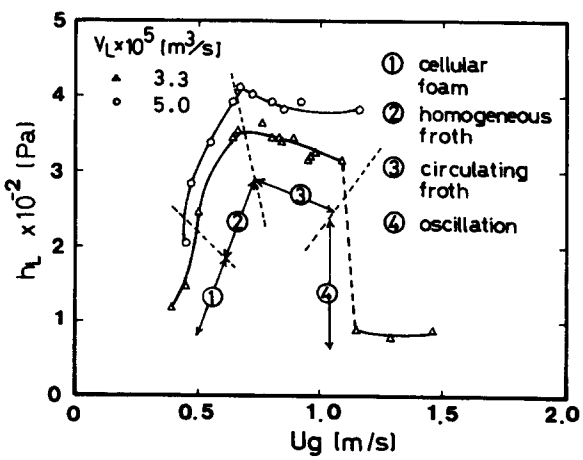

Figure 3. Clear liquid head as a function of superficial gas velocity (tray I).

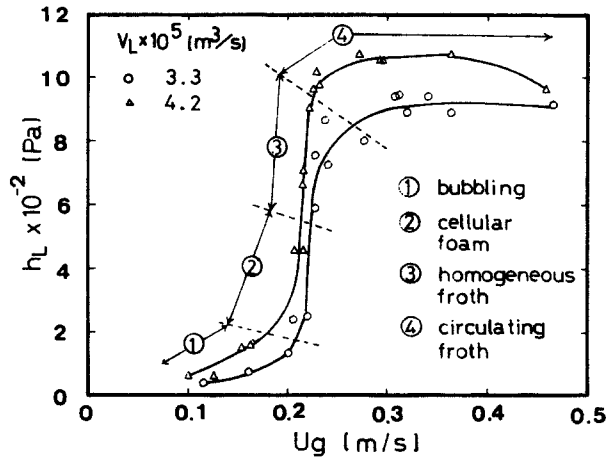

Figure 4. Clear liquid head as a function of superficial gas velocity (Tray II).

4.2 *Statistical properties of froth pressure fluctuations*

4.2.1 *Standard deviation.* The standard deviation of froth pressure drop σ_p with tray II, which represents the intensity of fluctuations, is shown in figure 5 as a function of average liquid hold-up. It can be seen from the figure that the cellular foam regime exhibits the smallest variation. For homogeneous and circulating froth regimes, the deviation was correlated by

$$h_L = 5.21 \exp(0.461\sigma_p) \qquad [1]$$

which resembled to Shoukry *et al.*'s (1974a).

4.2.2 *Autocorrelation function.* Figures 6–9 show the autocorrelation function r_k for different regimes. The bubbling regime exhibits strong periodicity, the dominant component of which is about 0.07–0.08 sec. In the cellular foam regime, the autocorrelation function damps out very quickly showing a wide band random noise, and thus can be distinguished from the bubbling regime. The homogeneous froth regime shows a similar feature, though a rather weak periodic component is embedded in a random background. In the circulating froth regime, the existence of periodicity with low frequency, about 2 Hz, is obvious. The result with tray I also indicated similar feature for each regime, which was omitted here.

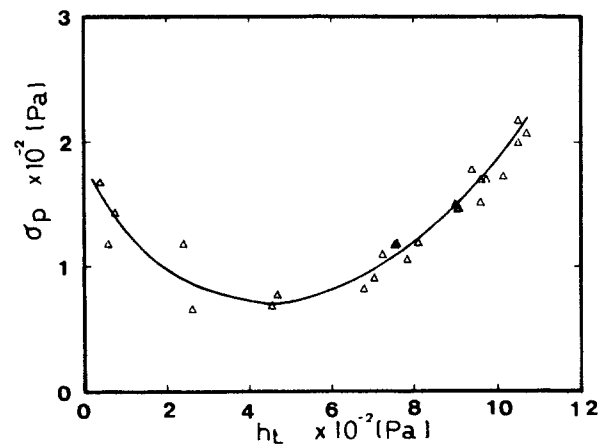

Figure 5. Relation between standard deviation of froth pressure drop and clear liquid head (tray II, $V_L = 4.2 \times 10^{-5}$ m³/s).

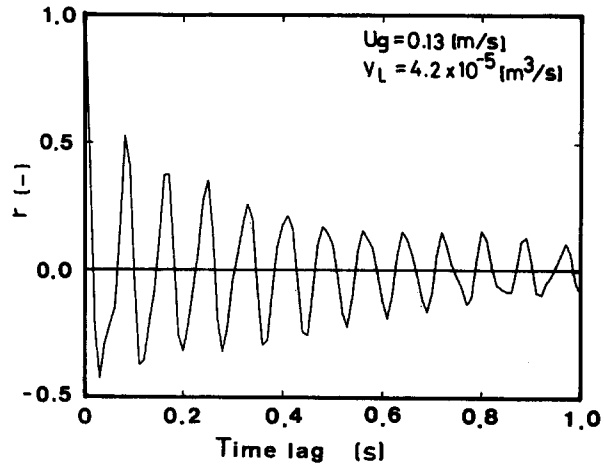

Figure 6. Autocorrelation function for bubbling foam regime (tray II).

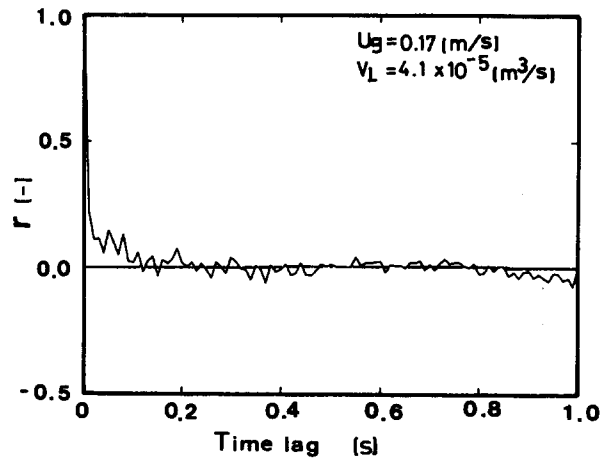

Figure 7. Autocorrelation function for cellular foam regime (tray II).

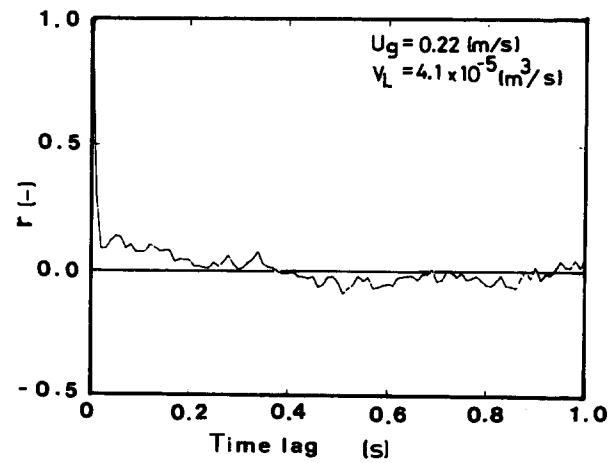

Figure 8. Autocorrelation function for homogeneous froth regime (tray II).

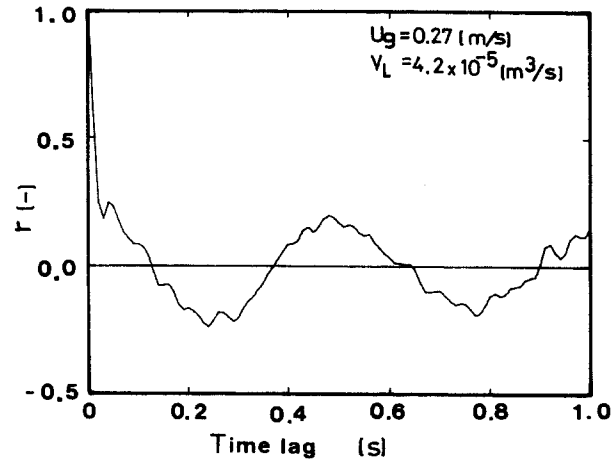

Figure 9. Autocorrelation function for circulating froth regime (tray II).

4.2.3 *The power spectral density function.* This function is a frequency-domain description of time series and appropriate for detection of frequency component embedded in the random process. The estimates of power spectral density functions $G(f)$ with tray II are illustrated in figures 10–13, where estimations by MEM are also shown by dotted lines. As compared with FFT method, the spectrum based on the MEM, generally, provides smooth curve removing violent variations, but longer computing time is needed. The MEM has also another weak point that there is no definite algorithm to determine the order of prediction error filter. Although there exists the minimum FPE procedure, this is not always almighty. Actually in this investigation, it was sometimes observed that the MEM spectrum exhibited very small number of peaks because of extremely small order of prediction error filter based on the FPE criterion.

Power spectrum in the bubbling regime, figure 10, indicates a strong peak at frequencies from 12 to 14 Hz which corresponds to the frequency of gas bubble generation. The cellular foam regime shows small power spread over a wide range of frequency except for relatively strong peaks at a smaller frequency range less than 2 Hz, which seems to represent a slow oscillation of clear liquid on the plate observed. In the homogeneous froth regime, the power spectrum indicates a major peak at around 1 Hz and larger power at other frequency range compared with those in the cellular foam regime. The oscillating regime has a dominant power at about 2 Hz corresponding to the frequency of the

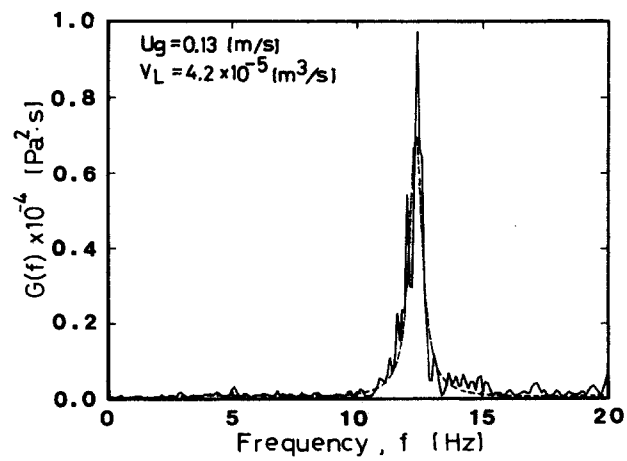

Figure 10. Power spectral density function for bubbling regime (tray II).

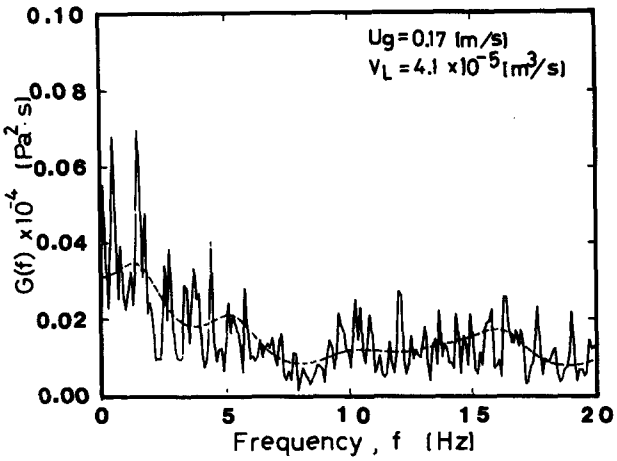

Figure 11. Power spectral density function for cellular foam regime (tray II).

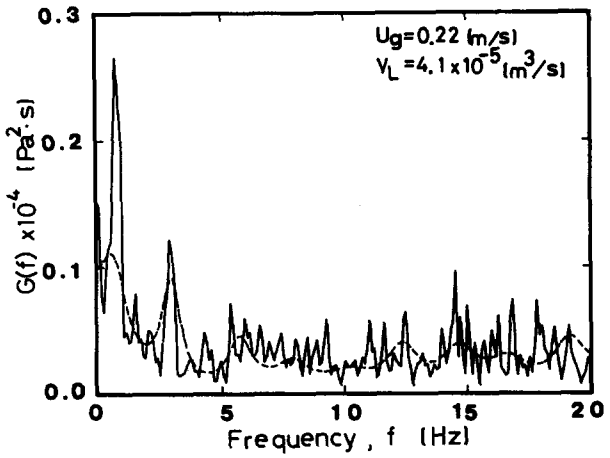

Figure 12. Power spectral density function for homogeneous froth regime (tray II).

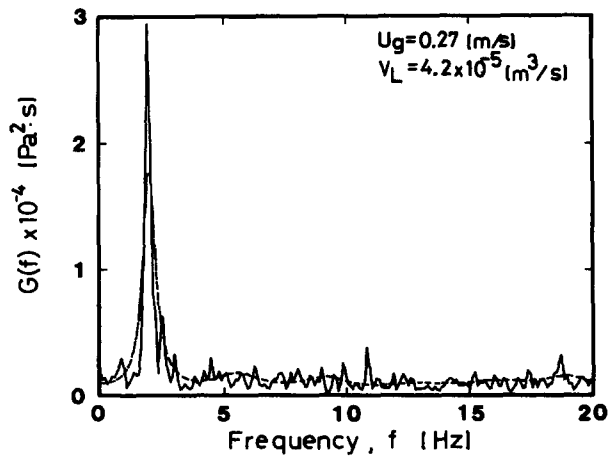

Figure 13. Power spectral density function for circulating froth regime (tray II).

macroscopic periodic oscillations of the froth. This was already obtained from the autocorrelation function.

Through the above examination, it is found that the power spectral structure of each hydrodynamic regime is distinctive, and hereby it may be possible to estimate the hydrodynamic regime of the gas–liquid dispersion on the plates from the measured data of power spectrum.

4.3 *Pattern recognition of the power spectra*

To realize the on-line estimation of the hydrodynamics of the froth by use of power spectra, it is necessary to establish an on-line recognition procedure of the spectral pattern. In this article, the following algorithm is proposed, which is illustrated as flow-chart in figure 14. To estimate the power spectrum density function, FFT method is adopted for reasons of its effective computing time. The estimated power spectrum is smoothed by using Hanning window twice so as to reduce the estimation error due to FFT method. Next, focusing on a frequency range up to 20 Hz, the spectrum is normalized so that the integration of the spectrum over 0 to 20 Hz becomes unity. Then, the frequency range over 0 to 20 is divided into 40 classes at an interval of 0.5 Hz, and then the mean value of power in each class is used as a representative of individual class. Thus the sample spectrum is represented by 40 discrete values. Finally, these spectra are classified by the criterion shown in figure 14. The criterion is independent of liquid flow rate over the range covered in this investigation.

The test of the algorithm with actual data was successful, which showed almost perfect recognition except for the transition regions. The feature of this procedure is that the

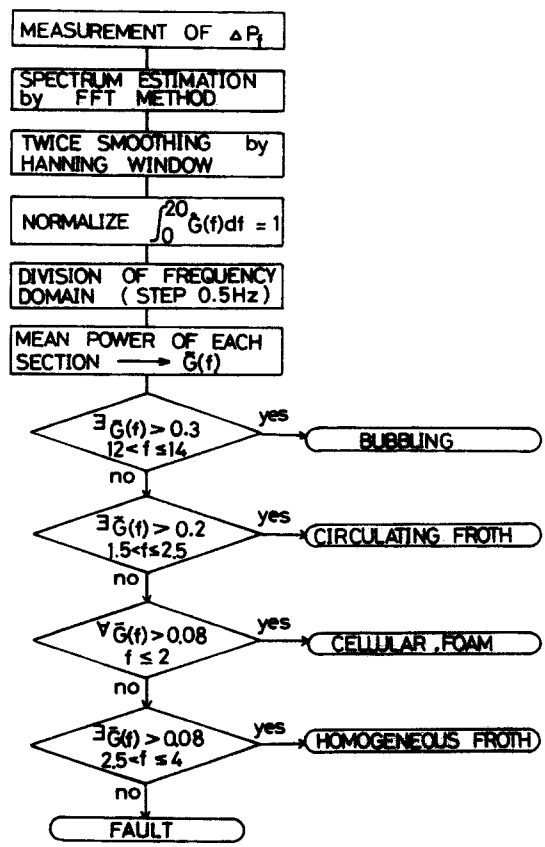

Figure 14. Procedure for flow regime estimation on the basis of pattern recognition of power spectral density functions.

algorithm is so simple as to be easily realized by means of usual spectral analyser on the market.

4.4 *Stochastic model of pressure fluctuations of froth*

The stationary models for time series, such as AR and ARMA, of fluctuations of froth pressure drop, were built, which are needed to achieve the optimal forecasting and control. The models identified for each regime are summarized in table 1. Figure 15 shows the comparison of the predicted values based on the model for bubbling regime with actually observed values. It can be seen from the figure that the model simulates well the actual behavior of fluctuations of the froth pressure drop. Consequently, these models may be applicable to implement a controller.

5. CONCLUSIONS

Statistical properties of hydrodynamics of gas–liquid dispersion on the plate were studied by using three plates column without downcomers for two different free areas, and these were characterized by the spectral structure of the fluctuations of froth pressure drop. The algorithm for pattern recognition of the spectra was proposed and tested successfully, so that it might be applied to the on-line estimation of hydrodynamics of the tray without

Table 1. Identified stochastic models of froth pressure fluctuations

Flow regime	Model type	Model	σ_a^2
Bubbling	AR(10)	$z_t + 0.416z_{t-1} - 0.186z_{t-2} - 0.273z_{t-3} + 0.128z_{t-4} - 0.114z_{t-5} - 0.176z_{t-6} + 0.073z_{t-7} + 0.252z_{t-8} - 0.026z_{t-9} - 0.157z_{t-10} = a_t$	0.467
Cellular foam	ARMA(3,1)	$z_t + 1.157z_{t-1} - 0.263z_{t-2} + 0.094z_{t-3} = a_t + 0.990a_{t-1}$	0.578
Homogeneous froth	ARMA(4,1)	$z_t + 0.297z_{t-1} - 0.045z_{t-2} - 0.027z_{t-3} + 0.125z_{t-4} = a_t + 0.095a_{t-1}$	0.996
Circulating froth	AR(3)	$z_t + 0.677z_{t-1} - 0.256z_{t-2} + 0.086z_{t-3} = a_t$	0.272

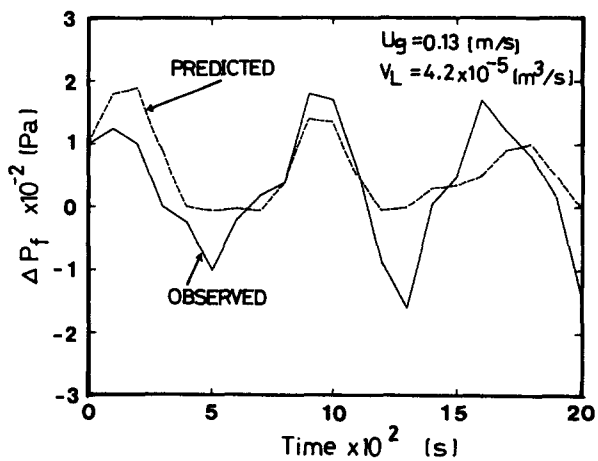

Figure 15. Comparison between predicted and observed fluctuations of froth pressure for bubbling regime.

visual inspection. Stochastic models for fluctuations of pressure drop across the tray were identified for several hydrodynamic regimes, and the possibility was verified of the time-domain prediction of fluctuations on the basis of the model.

Acknowledgements—The authors wish to express their gratitude to Messrs. K. Suzuki, K. Okamoto and Y. Yamashita for their assistance in the experimental work.

NOMENCLATURE

a_t white noise process
C_k estimate of kth lag autocovariance
f frequency
$G(f)$ estimate of power spectral density function
h_L clear liquid height on the tray
k number of lag
N number of time series data
p order of AR process
ΔP_f pressure drop across the gas–liquid dispersion
q order of MA process
r_k estimate of kth lag autocorrelation
Δt sampling time
U_G superficial gas velocity
V_L liquid flow rate
x_t time series data
z_t time series deviation from the mean value

Greek symbols

σ_a^2 variance of white noise process
σ_p standard deviation of froth pressure fluctuations

REFERENCES

AKAIKE, H. & NAKAGAWA, T. 1972 *Statistical Analysis and Control of Dynamical Systems*, pp. 50–92. Saiensu-sha, Tokyo (in Japanese).

AKAIKE, H. 1976 Canonical correlation analysis of time series and the use of an information criterion. *System Identification: Advances and Case Studies* (Edited by MEHRA, R. K. & LAINIOTIS, D. G.), pp. 27–96. Academic Press, New York.

BENDAT, J. S. & PIERSOL, A. G. 1971 *Random Analysis and Measurement Procedures*. Wiley, New York.

BIDDULPH, M. W. & STEPHENS, D. J. 1974 Oscillating behavior on distillation trays. *AIChE J.* **20**, 60–67.

BOX, G. E. P. & JENKINS, G. M. 1970 *Time Series Analysis: Forecasting and Control*. Holden-Day, San Francisco.

HINO, M. 1977 *Spectral Analysis*, pp. 83–236. Asakura-shoten, Tokyo (in Japanese).

JENKINS, G. M. & WATTS, D. G. 1968 *Spectral Analysis and its Applications*, pp. 310–317. Holden-Day, San Francisco.

SHOUKRY, E., CERMAK, J. & KOLAR, V. 1974a On the hydrodynamics of sieve plates without downcomers: I Dynamic nature of the gas–liquid dispersions. *Chem. Engng J.* **8**, 27–40.

SHOUKRY, E. & KOLAR, V. 1974b On the hydrodynamics of sieve plates without downcomers: II A model of plate operation and the phenomenon of multiplicity of steady state. *Chem. Engng J.* **8**, 41–51.

APPENDIX I

Evaluation of the statistical parameters

(1) *Autocorrelation function.* For N observations of ergodic stationary time series $x_1, x_2, \ldots, x_N$, the autocorrelation function r_k is estimated by

$$r_k = \frac{C_k}{C_0} \qquad [A1]$$

where

$$C_k = \frac{1}{N}\sum_{t=1}^{N-k}(x_t - \bar{x})(x_{t+k} - \bar{x}), \qquad k = 0, 1, 2, .., K \qquad [A2]$$

is the estimate of autocovariance, and $\bar{x}$ is the mean of the time series.

(2) *Power spectral density function.* The power spectral density function was estimated by FFT algorithm and MEM described below. The MEM spectrum is expressed by

$$G(f) = \frac{\Delta t \sigma_z^2}{\left|1 + \sum_{k=1}^{p} \phi_k \exp(i2\pi f k \Delta t)\right|^2} \qquad [A3]$$

where Δt is the sampling time, ϕ_k are the coefficients of the following Yule–Walker equations,

$$\begin{aligned}
&C_0 + \phi_1 C_1 + \phi_2 C_2 + \cdots + \phi_p C_p = \sigma_z^2 \\
&C_1 + \phi_1 C_2 + \phi_2 C_3 + \cdots + \phi_p C_{p-1} = 0 \\
&\cdots\cdots\cdots\cdots\cdots\cdots \\
&C_p + \phi_1 C_{p-1} + \phi_2 C_{p-2} + \cdots + \phi_p C_0 = 0 \\
&C_{p+1} + \phi_1 C_p + \phi_2 C_{p-1} + \cdots + \phi_p C_1 = 0
\end{aligned} \qquad [A4]$$

and σ_a^2 is the variance of prediction error.

APPENDIX II

Identification of stochastic model

The order of the stationary model such as AR and ARMA was determined on the basis of the following two methods developed in recent years. According to the FPE (Final Prediction Error) criterion (Akaike & Nakagawa 1972), the best model is the one which provides the minimal FPE defined by

$$\text{FPE} = E[(x_t - \hat{x}_t)^2] \qquad [A5]$$

where $\hat{x}_t$ is a predicted value by the model. Especially for AR(p) model, the FPE is described by

$$(\text{FPE})_p = \left\{1 + \frac{p+1}{N}\right\}\left\{1 - \frac{p+1}{N}\right\}^{-1}\sigma_a^2 \qquad [A6]$$

where σ_a^2 is the estimated variance of white noise process and N is the length of data. For ARMA(p, q) model, the minimum AIC procedure (Akaike 1976) can be used, which

intends to minimize the AIC defined by

$$\mathrm{AIC} = N \log (\sigma_a^2) + 2(p + q) \qquad [A7]$$

where σ_a^2 is the estimated variance of white noise process and p and q are, respectively, order of AR and MA process. The model parameters were determined by the least square estimation.